Wireless wearable wristband for continuous sweat pH monitoring

Pablo Escobedo,[e] Celia E. Ramos-Lorente,[a] Antonio Martínez-Olmos,[b,d] Miguel A. Carvajal,[b,d] Mariano Ortega-Muñoz,[c,d] Ignacio de Orbe-Payá,[a,d] Fernando Hernández-Mateo,[c,d] Francisco Santoyo-González,[c,d] Luis F. Capitán-Vallvey,[a,d] Alberto J. Palma,[b,d] Miguel M. Erenas[a,d]

[a] *ECsens, Department of Analytical Chemistry, Faculty of Sciences, Campus Fuentenueva s/n, University of Granada, 18071-Granada, Spain*
[b] *ECsens, Department of Electronics and Computer Technology, ETSIIT C/Pta. Daniel Saucedo Aranda s/n, University of Granada, 18071-Granada, Spain.*
[c] *Department of Organic Chemistry, Biotechnology Institute, Faculty of Sciences, Campus Fuentenueva s/n, University of Granada, 18071-Granada, Spain*
[d] *Unit of Excellence in Chemistry applied to Biomedicine and the Environment of the University of Granada.*
[e] *Bendable Electronics and Sensing Technologies (BEST) Group, University of Glasgow, Glasgow, G12 8QQ, UK*

Abstract

Several studies have shown that the determination of pH in sweat, which is one of the most accessible body fluids, can be an indicator of health and wellness, and even be used for potential disease diagnosis. On that basis, we present herein a wearable wristband for continuous and wireless monitoring of sweat pH with potential applications in the field of personal health assessment. The developed wristband consists of two main parts: a microfluidic cloth analytical device (μCAD) to collect continuously the sweat from skin with a color-based pH sensing area; and a readout and processing module with a digital color sensor to obtain the pH of sweat from the color changes in the μCAD. In addition, the readout module includes a low-power Bluetooth interface to transmit the measurements in real-time to a custom-designed smartphone application. To allow continuous operation, an absorbent pad was included in the design to retire and store the sweat from the sensing area through a passive pump path. It was found that the Hue parameter (H) in the HSV color space can be related to the sweat pH and fitted to a Boltzmann equation (R^2=0.997). The range of use of the wristband device goes from 6 to 8, which includes the pH range of sweat, with a precision at different pH values from 3.6 to 6.0 %. Considering the typical human sweat rate, the absorbent pad allows continuous operation up to more than 1000 minutes.

Keywords: pH sensor; Sweat analysis; Microfluidic cloth analytical device (μCAD); Wearable system; Wireless monitoring; Smartphone.

1. Introduction

Wearable technology has significantly evolved in the last years with the advent of products such as smartwatches and wristbands. In particular, the use of wearables for personal health assessment has fuelled the growth of these devices by enabling non-invasive methods for continuous monitoring of physical activity and vital signs [1,2]. Not surprisingly, the wearable fitness technology market was valued at $5.77 billion in 2016 and it is expected to be worth $12.44 billion by 2022, growing at an estimated compound annual growth rate (CAGR) of 13.7% from 2016 to 2022 [3]. Among the different physiological parameters of interest, we must highlight the monitoring of heart rate [4], blood pressure [5,6], respiration rate [7], body temperature [8] and sweat [9–12]. In contrast with traditional health monitoring instruments, wearable devices have some key advantages such as portability, ubiquity or ease of use, and they are able to provide continuous, real-time, wireless monitoring of health conditions in a non-invasive way [13–16].

Several studies have shown that analytes of interest in blood such as glucose, lactate, urea or sodium, to name but a few, are also found in other biofluids sources such as saliva, tears or sweat [17]. The main advantage of using these alternative biofluids lies in their easier access, thus avoiding the need for acquiring blood samples and allowing peripheral biochemical monitoring [18,19]. Sweat is particularly attractive since it is one of the most accessible body fluids, and it can even be produced by on-demand stimulation using techniques such as iontophoresis [20]. pH determination in sweat is an indicator of health and wellness, and it can be used even for potential disease diagnosis. Under normal conditions, the pH of healthy human sweat is within the range from 4.5 to 7.0. Nevertheless, the pH of our sweat can vary dramatically under circumstances of homeostasis dysregulation, disease, acidosis and even stress [21]. For instance, cystic fibrosis patients are reported to have a higher pH (up to pH 9) than normal individuals [22], and sweat pH can be also used as an indicator of metabolic alkalosis [23]. In the field of sport and exercise, it is well known that the formation and evaporation of sweat is the principal means of heat removal. If the sweat losses lead to a body water deficit or hypohydration, the reduced volume of body fluids will contain a greater concentration of sodium (Na^+) and potassium (K^+), which can cause hypertonic hypovolemia [24]. Severe dehydration can lead to headache, vomiting, muscle cramping, dizziness, nausea and even fainting. In this context, sweat pH can be used to monitor exercise intensity and dehydration since it is associated with sodium concentration [25]. On the other hand, excessive water intake can cause hyponatremia, which refers to a low sodium concentration. Clinical features of symptomatic hyponatremia include seizures, pulmonary edema, muscle fasciculation, disorientation, mental confusion, respiratory arrest, weakness, nausea and even coma [26]. Therefore, the reliable monitoring of sweat pH is crucial for health assessment and wellness monitoring applications [27].

Different approaches for wearable sweat pH monitoring can be found in the literature over the last few years. According to their sensing strategy, a number of

platforms draw upon optical colorimetric detection [10,28–32], while others make use of electrochemical pH sensors [31,33,34] reviewed by Chung et al. [19]. In the first case, the use of microfluidic devices allows the precise positioning of the reagents in a specific test zone to which the sweat is guided, thus taking place the desired reaction with the subsequent color change [35].

The study of the evolution on time of sweat both rate and composition in different areas of the body has been approached in two main ways referred to passive sampling: *i)* microchannel-based microfluidics that rely on deterministic capillary, the so-called capillary microfluidic [36]. In this case, epidermal microfluidic systems that combine channels, valves, mixers, and reservoirs, are able to capture, route, and store microliters of sweat in a time-controlled manner [35]; or *ii)* porous capillary microfluidics that rely on stochastic capillary flow within a network of pores (paper, cloth, thread) in which the sweat is collected, and delivered to the sensing area being removed by an adsorbent acting as a passive pump [25].

To make the system truly wearable and portable, a wireless interface is required to transmit the measured data to the end user. Many systems include a Radiofrequency Identification (RFID) solution, usually a Near Field Communication (NFC) link [32,33,37]. This approach allows the development of passive systems by means of energy harvesting from the electromagnetic field of an external reader, typically an NFC-enabled smartphone. Moreover, the NFC antenna required for this design can be manufactured in flexible and conformable substrates, even stretchable [31,33]. However, this approach is not suitable for continuous, real-time sweat monitoring, since it requires that the external reader is permanently placed close to the system. To overcome such limitations, other systems employ longer range wireless technologies such as Wi-Fi [38,39] or Bluetooth [10,34,40].

In this work, we present a wearable wristband for sweat pH monitoring. As Fig. 1 shows, the system comprises two main parts: *i)* a custom-designed microfluidic cloth analytical device (μCAD) to collect and store the sweat that includes a color-based pH sensor built by immobilization of a vinyl sulfone acidochromic dye (AD-VS) on a cotton cloth; and *ii)* a miniaturized readout module to obtain the pH measurements from the sensor and extra circuitry to interface with the end user. The proposed wristband allows continuous monitoring of sweat pH and real-time wireless transmission of the measurements to a smartphone via Bluetooth. The presented system distinguishes from previous works in the same field by combining the following three main aspects: *i)* The development of a novel compound covalently immobilized in cloth optimized for optical pH sensing with high response speed; *ii)* The inclusion of an absorbent pad to retire and store the sweat from the sensing area through a passive pump path, which allows continuous operation up to more than 1000 minutes; and *iii)* The design of miniaturized and low-power electronics embedded with the sensing module in a compact and light-weight wristband design, which is completed by a custom-developed smartphone application for real-time monitoring.

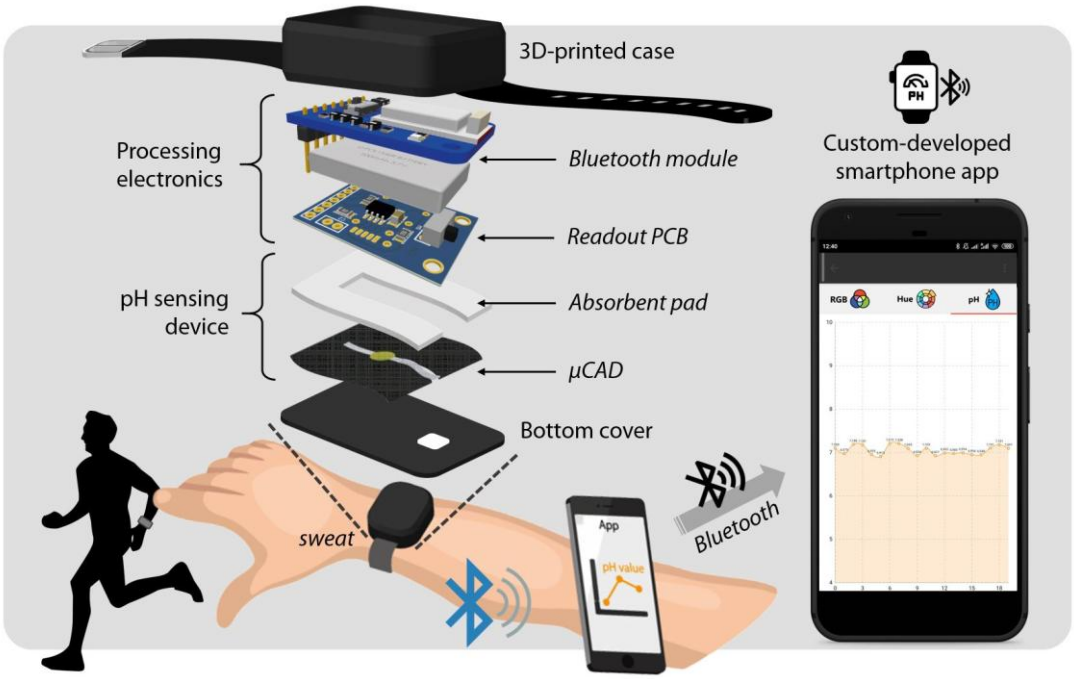

Fig. 1. Exploded view of the wireless wearable wristband, consisting of the custom-designed µCAD with a colorimetric pH sensor and a miniaturized readout module to obtain the pH information from the sensor. Real-time measurements of sweat pH are transmitted to the user smartphone via Bluetooth through a custom-developed app.

2. Materials and Methods

2.1. µCAD design and fabrication

All reagents and materials used for the µCAD preparation are detailed in Section S1 of the Electronic Supplementary Information (ESI), while the synthetic procedures of AD-VS-1 and its optical characterization are detailed in Sections S2 and S3, respectively. Firstly, a piece of 13.8×17.4 cm^2 of cotton cloth, previously characterized by us in terms of Washburn constant (see Section S4), was screen-printed using a 43 lines·cm^{-1} frame together with a black plastisol ink, to pattern 12 hydrophilic sections as shown in Fig. S9 of Section S5. Lately, the large piece of cotton cloth was cut to obtain each pattern independently, that will be used to prepare the µCAD. Once the cotton patterned cut was obtained, the vinyl sulfone acidochromic dye AD-VS-1 (Fig. 2(a)) was immobilized according to the following procedure. Firstly, it was introduced in a Na_2CO_3 10 mg·mL^{-1} solution for 1 h to scour the screen-printed fabric and improve its capillary properties, as well as to get a basic media on the cloth that makes possible the click immobilization of the AD-VS-1 via oxa-Michael addition by adding of 0.2 µL of AD-VS-1 15 mg·mL^{-1} in DMSO. Afterwards, the cloth was located in a light-safe and let dry for 24 h, and then washed to remove the excess of AD-VS-1 by sonication in Tris buffer pH=9.2, purified water and methanol, 10 minutes each. Finally, the µCAD was placed in the bottom of the designed holder and, on top of it, the U-shaped absorbent pad as shown in Fig. 2(b-c). The µCAD, as well as the U-shaped absorbent

pad, are disposable components that can be replaced when necessary. To collect the sweat, a piece of the sampling path passes through a hole at the bottom cover of the 3D-printed case, being in touch with the skin and collecting the sample while sweating.

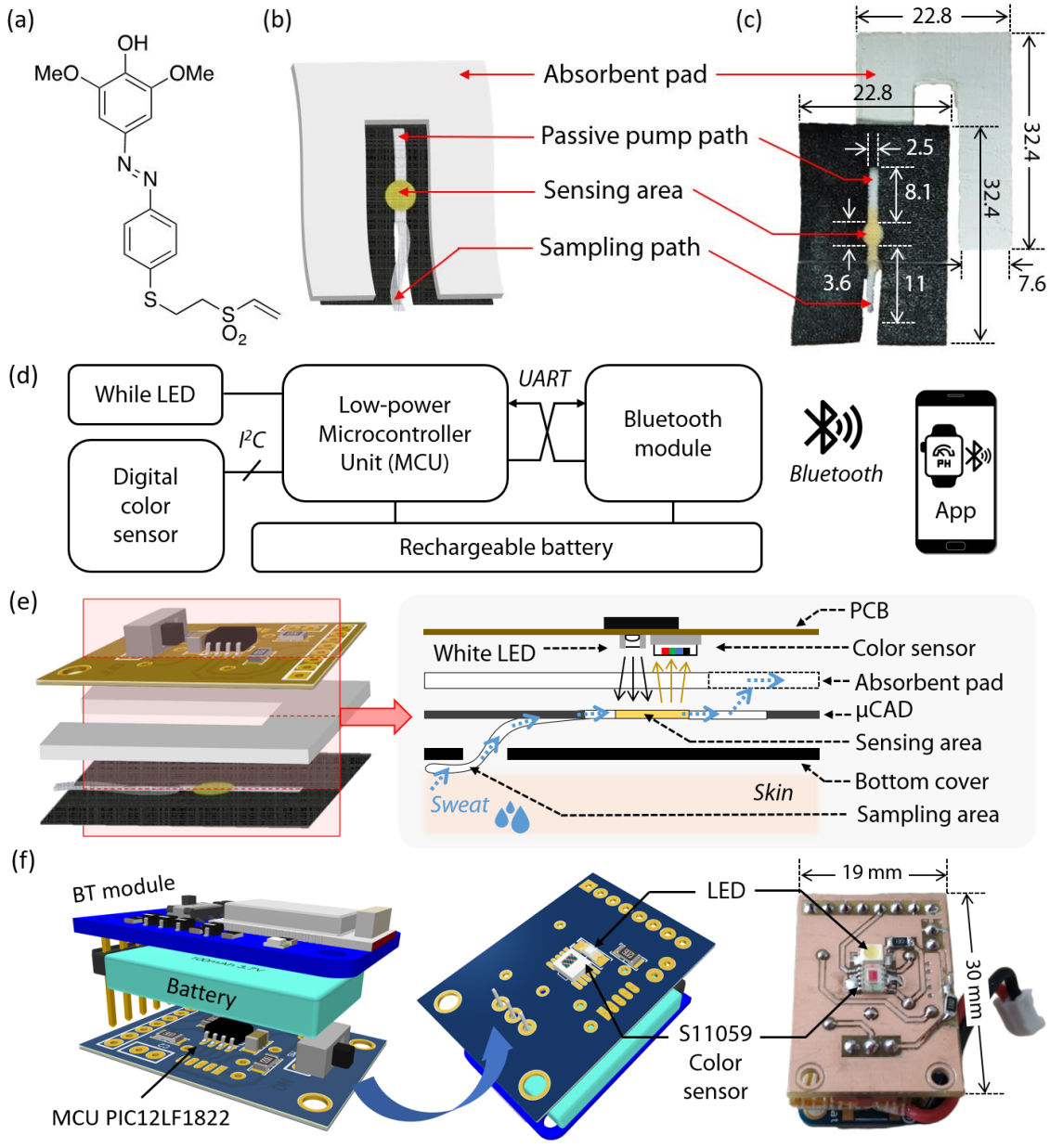

Fig. 2. (a) Chemical structure of AD-VS-1; (b) µCAD design; (c) µCAD photograph; (d) Block diagram of the processing electronics in the readout module; (e) Schematic diagram of the sensing procedure in which the LED and color sensor are placed in front of the sensing area of the µCAD; (f) 3D views and real image of the fabricated module with its main components labelled.

In humans, the rate of sweating is around 1250 $g \cdot m^{-2} \cdot h^{-1}$ when exercising [41]. For that reason, both the sampling and the sensing areas in the µCAD design had to be small enough to avoid the need of high volumes of sample. On the other hand, however, the

sensing area needed to have a minimum diameter of 3.6 mm so that the detector included in the device could perform reliable measurements. Cotton cloth was selected as the support for the µCAD because it presents better properties than paper in terms of flexibility and bending resistance. However, as it occurs with paper, the cotton cloth needed to be patterned to achieve that the sample and reagent flow through a specific path. For this reason, the designed pattern (Fig. 2) comprises of several parts: *(i)* a sampling zone were the sweat is recollected or added, *(ii)* a sensing area were the AD-VS-1 is immobilized, and *(iii)* a passive pump path in which the sample flows to reach *(iv)* an absorbent U-shaped material that makes it possible the use for a prolonged operation.

Before the optimization of the µCAD preparation, the analytical parameter used to characterize the color change of the immobilized AD-VS-1 was selected. For this purpose, several small cotton pieces were prepared as described in Section S6 and tested on pH solutions ranged from 4 to 9 (n=3), recording and analysing the color in the RGB and HSV color spaces (see Fig. S11). The Hue (H) parameter showed a higher color variation at lower pH with lower error bars reason by that was used for the study (see Fig. S12).

Once H was selected as analytical parameter and the µCAD was designed and fabricated, different parameters related to the immobilization of the AD-VS-1 were studied. Firstly, the volume that must be added to the sensing area was evaluated in order to cover the circle in a reproducible way. For this purpose, different volumes ranging from 0.1 to 0.5 µL of a Brilliant Blue solution (10 $mg \cdot mL^{-1}$) were added, being 0.3 µL the volume that best and most homogeneously covered the sensing area (see Fig. S13 in Section S7). Later, and based on the obtained results, the same test was performed using a 10 $mg \cdot mL^{-1}$ AD-VS-1 in DMSO solution to confirm these results. In this case, the volume that best covered the sensing area was 0.2 µL. The volume needed in this case was lower due to the used solvent, since Brilliant Blue solution was solved in water, while AD-VS was in DMSO and it affected to the wicking on cloth.

Later, the concentration of AD-VS-1 solution in DMSO was optimized. For this purpose, different AD-VS-1 solutions from 5 to 20 $mg \cdot mL^{-1}$ (see Section S7) were tested, resulting that 15 $mg \cdot mL^{-1}$ was the concentration that best results provided in terms of CV as well as pH range of variation of the signal, being the one whose H value changed at lower pH (see Section S8).

Finally, two different procedures to prepare the µCAD were assayed (see Section S9). In the first procedure, the cloth was first patterned and later the reagent was immobilized. In the second procedure, these steps were followed in reverse order. The obtained results (see Fig. S15) proved that the procedure providing best results in terms of reproducibility was the patterning followed by the immobilization of the AD-VS-1.

2.2. Readout and processing electronics

The readout module comprises as main electronic components a low-power microcontroller unit (MCU) model PIC12LF1822 (Microchip Technology Inc., Chandler, Arizona, USA); a Bluetooth module Bluefruit Low Energy (BLE) UART

Friend (Adafruit, New York, USA); a high-resolution digital color detector model S11059-02DT (Hamamatsu Photonics, Japan); a white excitation LED; and a rechargeable battery of 3.7 V and 150 mA·h capacity model JJR/C H36-004 (Goolsky, Singapore, Asia). Fig. 2(d) shows the block diagram of the processing electronics.

The sensing module, which comprises of the excitation LED and the color detector, is placed aligned in front of the pH-sensitive membrane, as shown in Fig. 2(e). The selected color detector S11059-02DT is sensitive to red (λ_{peak}=615 nm), green (λ_{peak} =530 nm), blue (λ_{peak} =460 nm), and near infrared (λ_{peak} =855 nm) incident radiation, codifying it in four 16-bit digital words. These words are sent to the MCU by means of an I^2C interface for further processing. The excitation LED is synchronised with the reading protocol of the color detector. The selected LED is white since the parameter to be determined is the color of the sensitive membrane. After the processing, the MCU sends the data to the Bluetooth module via Universal Asynchronous Receiver-Transmitter (UART) protocol. The processed data is then wirelessly transmitted to a mobile phone via Bluetooth. Fig. 2(f) shows the 3D views and real image of the fabricated readout module.

A 3D-printed case was designed and composed of two pieces fitting each other and manufactured with coal black polylactic acid (PLA) and polyurethane Filaflex. In this way, we ensure the correct alignment and positioning of the pH sensor with respect to the LED and color detector, while providing a uniform dark environment for the color measurements. More details about the design and fabrication of the 3D-printed case can be found in Section S10. In addition, to transmit the data in real-time from the wristband to the user, a custom-designed Android™ application was developed. The application takes control of the Bluetooth interface of the smartphone to communicate with the Bluefruit LE module. Once the wristband is paired with the smartphone, the BLE sends in real time the measured color data obtained through the color sensor (in RGB coordinates) from the MCU to the app. The RGB coordinates are then converted to the H value in the HSV color space. Finally, the pH values are computed from the normalized H values as per the obtained calibration, and the graph is displayed on the screen. The application includes a datalogger function and the results can be shared through email and/or different cloud or messaging services, thus allowing the possibility to connect to remote health care providers or medical experts. More details regarding the development and some screen captures of the application can be found in Section S11 of ESI.

3. Results and Discussion

3.1. Selection, synthesis and characterization of the acidochromic dye indicator AD-VS-1

Parallel advances in chemical sensing and wireless communication technologies have sparked the development of wireless chemical sensors. In this work, our engineering design is based on the use of μCAD as an optical sensor for the detection

and determination of pH as the analyte. In this respect, acidochromism evolved for the sensing area of the µCAD by means of an immobilized acidochromic indicator dye as a recognition element was thought to be an adequate methodology [42]. Among the different suitable dyes, our selection was based in the appealing features of vinyl sulfone azo dyes (AD-VS). These compounds combine the outstanding optical properties of azo chromophores with the relatively high reactivity of the vinyl sulfone group (VS) [43,44]. The reactivity of the VS functional group fulfils most of the essential requirements needed for covalent immobilization of the azo dye to cotton cloth as the support of choice for the µCAD fabrication: *(i)* a complementary reactivity with the intrinsic nucleophilic OH present in cellulose that react by a Michael-type addition, *(ii)* a high stability of the resulting ether link, *(iii)* it takes place in an aqueous milieu, and *(iv)* a simplified one-step procedure that minimize the operational. On the base of these outstanding features AD-VS have found application in textile chemistry [45] and they also have demonstrated their value in the fabrication of devices for optical pH sensing [42,46–48].

Considering the current state-of-the-art, we decided to prepare a novel member of this family of compounds, named AD-VS-1 (Fig. 2(a)), as suitable for our purposes. We envisaged an easy strategy based in a straightforward two-step procedure that starts from 4-aminothiophenol (see Section S2). After treatment of this aromatic compound with divinyl sulfone, that led exclusively to the corresponding thia-Michael reaction addition intermediate due to the higher nucleophility of the sulfur atom respecting to the amino group, concomitant diazotation reaction with 2,6-dimethoxyphenol afforded the desired AD-VS-1. Spectroscopic characterization of this indicator dye confirms this molecular structure, whose optical profile (absorbance spectra and molar extinction coefficient in DMSO solution) was also determined (see Section S3).

3.2. µCAD and pH sensor performance

As can be observed in Fig. 2(b-c), the hydrophilic section of the µCAD is composed by a sensing area and two paths: the sampling path (2.5 mm x 11.0 mm) and the passive pump path (2.5 mm x 8.1 mm). A 2.5-mm wide path was selected since it was the narrowest path that could be screen-printed on the cloth in the reproducible way. The length of both paths, sensing area size, and position in the 22.8 mm x 32.4 mm piece of cloth used to fabricate the µCAD, were selected based on the Printed Circuit Board (PCB) and 3D-printed case design.

After the µCAD design and optimization, a calibration was conducted by dipping the µCADs in 10 different standard solutions with pH from 4 to 10 during 30 s in each solution (see Section S12). Six different µCAD were used for the calibration. In three of them, the calibration was conducted by rising the pH value of the standard solution, while in the other three cases the pH was diminished during the calibration. This strategy was chosen to prove that the obtained H value was independent from the pH variation direction. As it can be observed in Fig. S18, the obtained results were

independent from the rising or diminishing of the pH value, so the six replicates were used to obtain a Boltzmann equation fitting the data set (R^2=0.997) (see Fig. S19).

The results of this first study indicate that the designed µCAD can be used to determine the pH of sweat with good precision and within the range of the sample. However, at this stage it cannot be claimed yet that the µCAD could be used for real-time determination of pH sweat. The reason behind this is that the µCAD hydrophilic area is so small that it will be full of sample in a very short period of time. Because of that, some material needed to be included for the purpose of continuously retiring sample from the hydrophilic area of the µCAD to allow that new sample could continue flowing through it. This would ensure that the µCAD could be used during longer periods of time before saturating. The strategy followed was the inclusion of a passive pump in the µCAD, along with an absorbent pad containing Flexicel (P&G Spain, Madrid) skirting the hydrophilic area (see Fig. 2(b-c)). Flexicel is a superabsorbent material whose characterization is shown in Section S13. According to the slope of the calibration function in Fig. S20(a), this material can absorb around 20 times its weight. This material has been successfully used as passive pump in other microfluidic devices that can be found in the literature [49]. The area of the absorbent pad used in our design was 689 mm^2. Based on the calibration of the material and considering a sweat rate of 0.01 $\mu L \cdot s^{-1}$ (in around 15 mm^2 area) [41], the µCAD along with the absorbent pad could be used continuously up to 1058 min. Size and shape of the absorbent material was selected based on the 3D-printed case, to be easy-to-place inside while maintaining its position inside during the use of the device.

A new calibration was conducted, on this occasion with the µCAD including the passive pump. In this case, a syringe pump was used to apply the sample on the sampling zone (see Fig. 2(b)) at a flow rate similar to the human sweat rate (0.01 $\mu L \cdot s^{-1}$). Each pH standard solution was applied to the µCAD during two minutes and videotaped. From the obtained results (see Fig. S21 in Section S14) it can be observed that only 90 seconds were enough to get a steady signal, which was used to obtain the calibration function (see Fig. 3). The data fits as previously described to a Boltzmann equation (R^2=0.996) (Eq. S2), and the range of use of the µCAD is from 6.1 to 8.4 (pKa=7.4), range in which the pH of sweat is included. The precision tested at different pH goes from 2.3 to 3.6 % (see Table 1).

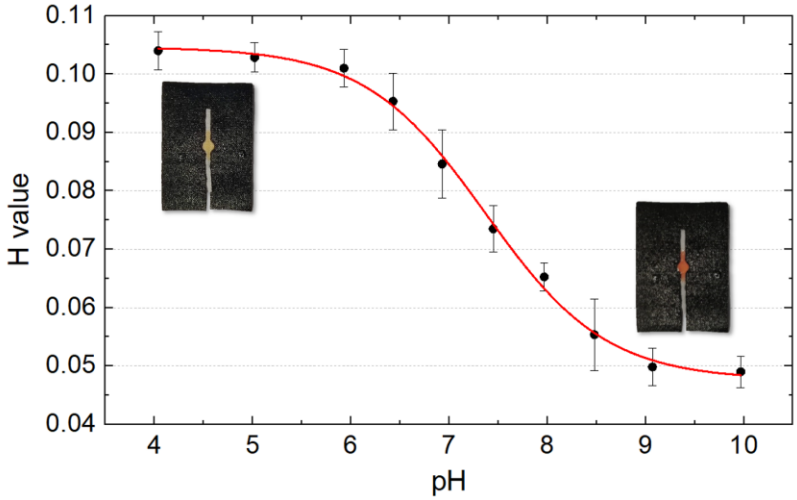

Fig. 3. Calibration curve of the µCAD including the passive pump, where the standard pH solutions were applied on the sampling zone using a syringe pump at a rate of 0.01 $\mu L \cdot s^{-1}$, which is similar to the human sweat rate.

Table 1. Analytical parameters of µCAD.

Analytical parameters			
$\mathbf{A_1}$	0.104	**Precision (n=10)**	
$\mathbf{A_2}$	0.047	**pH**	**CV (%)**
$\mathbf{A_3}$	7.372		
$\mathbf{A_4}$	0.614	4.04	2.5
$\mathbf{R^2}$	0.996	7.45	3.5
LOD	6.1	7.97	2.3
Range	6.1 - 8.4	9.97	3.6

Due to the nature of the sweat sample, whose pH can rise or diminish indistinctly during an exercise session, an additional study was conducted (see Section S14) to prove that the µCAD is fully reversible to pH variations. Fig. S22 shows that the µCADs are fully reversible after subjecting them to a cycle of acidic-basic-acidic pH and basic-acidic-basic pH, respectively. Finally, a stability study included in Section S15 was performed by observing the H value of three different µCADs along 20 weeks. This study showed that, once prepared, the µCAD can be stored for 7 weeks (Fig. S23). Once the µCAD was fully characterized, seven different samples were analysed using the µCAD and the obtained results were compared to the ones provided by a pH-meter (Section S16).

3.3. Wristband performance and evaluation

As indicated in the previous section, the µCAD was analytically characterized for pH sensing and a calibration function was obtained using a camera to register the color variations (see Fig. 3). At this stage, the whole system was characterized using the

optimized µCAD in combination with the readout and processing electronics. Thus, the way of registering the color changes in the µCAD due to the sweat pH was conducted through the digital color sensor included in the readout circuit (see Fig. 4(a-b)). For the calibration, a similar setup than the previous case was employed, i.e. a syringe pump was used to apply the sample on the sampling zone at a flow rate similar to the human sweat rate (0.01 $\mu L \cdot s^{-1}$). Each pH standard solution was applied to the µCAD during two minutes and the color measurements from the digital sensor were transmitted every second to the smartphone app via Bluetooth. Fig. 4(c) shows the obtained calibration curve, that can be again fitted to a Boltzmann curve (R^2=0.997) (Eq. S2). In this case, the range of use of the µCAD ranges from 6.0 to 8.0, and the precision at different pH values goes from 3.6 to 6.0 % (see Table 2). In addition, the system was tested in real-life conditions by wearing it on the wrist while exercising and transmitting the data in real-time to a smartphone via Bluetooth. Fig. 4(d) shows the experimental setup and the obtained results. Two different sections can be distinguished in this graph: *(i)* a priming section (0-7 min) that comprise the time to start sweating as well as wetting the fluidic channel and sensing area; and *(ii)* a pH-responsive section once the whole system is conditioned. Once the priming time has finished (vertical dashed line in Fig. 4(d)) the sampling area has changed its color due to the sweat pH. Considering the device calibration depicted in Fig. 4(c), which was conducted using pH standard solutions, we have highlighted in Fig. 4(d) some pH values in this section. At that point, the pH values stand at around 6.4 – 6.6, which is consistent with previous research works in this field [34,51].

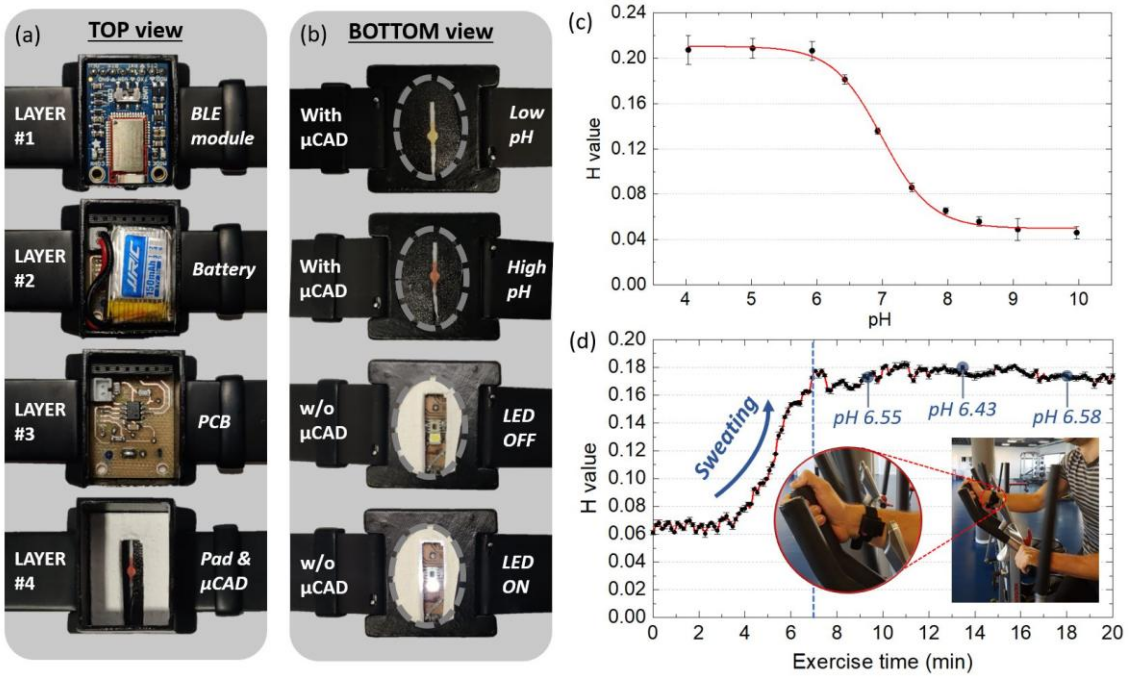

Fig. 4. (a) Layer by layer top view of the wristband, including: *1)* Low-Energy Bluetooth module, *2)* battery, *3)* PCB, and *4)* absorbent pad with µCAD; (b) Bottom view of the wristband (uncovered) with and without the µCAD layer to allow the view of the LED and color detector; (c) Calibration curve of the wristband wearable system in terms of H value; (d) Real-time results of the wearable system placed on the wristband during exercise.

Table 2. Analytical parameters of the wristband.

Analytical parameters			
A_1	0.210	**Precision (n=10)**	
A_2	0.050	**pH**	**CV (%)**
A_3	0.699	6.00	4.0
A_4	0.377	6.43	6.0
R^2	0.997	6.93	4.5
LOD	6.0	7.45	4.3
Range	6.0 - 8.0	7.97	3.6

Overall, the developed system is convenient in terms of portability, ease of use and wearability. With a total weight of 25 g (including the strap), which is in line with the most popular fitness wristbands such as the Fitbit Charge 4 (30 g), Garmin Vivosport (27 g), or Samsung Galaxy Fit (24 g), the developed wristband is light-weight and comfortable to wear. A number of previous works have focused on the development of sensing patches for sweat pH monitoring [18,25,28,30,52], but they lacked the associated readout and processing electronics to obtain and transmit in real-time the measured information to the end user. In contrast to the RFID/NFC-based platforms for pH sweat sensing than can be found in previous literature [15,31,37], our proposed wristband does not require that the external reader is permanently placed in its close proximity, thus allowing a truly continuous real-time monitoring. In return, our system requires a battery for its operation, which is not needed in the case of RFID/NFC devices with energy harvesting capabilities [33]. However, the use of low-power components in combination with the non-continuous measurement strategy allows a long battery life of more than 2 days. More details regarding the electronics performance and battery life can be found in Section S17. In terms of response speed, our system only takes 90 seconds to get a steady signal in the sensing zone through the use of the passive pump to collect the sweat, which is significantly lower than the time required in other systems to get the first readings [9]. Besides, the proposed wristband is distinguished from previous sweat pH monitoring systems in two more aspects: firstly, it features a very compact and light-weight design with a size similar to a wristwatch, making it more comfortable to use than other devices that must be placed, for instance, in the back; and secondly, it is completed by a custom-developed user-friendly smartphone application [10,28,34,40].

4. Conclusions

A wearable wristband for sweat pH wireless monitoring was developed combining a custom-designed μCAD and associated readout and processing electronics. The μCAD was designed in 100% cotton cloth by immobilizing an acidochromic dye (AD-VS-1). The μCAD consists of a sampling area to collect the sweat, a colorimetric sensing area, a passive pump path, and an absorbent pad that allows continuous operation up to 100

min if we consider a typical human sweat rate (0.01 $\mu L \cdot s^{-1}$). The H value in the HSV color space was selected as the best parameter to correlate the color change in the sensing area due to the pH variations. The readout module consists of a low-power microcontroller unit that controls a white LED and a digital color sensor to detect the color variations in the μCAD sensing area. In addition, a Bluetooth module transmits in real-time the measurements to a friendly-user smartphone application. The analytical characterization of the μCAD alone showed that the H parameter can be related to the sweat pH value and fitted to a Boltzmann equation (R^2=0.996). The range of use of the μCAD goes from 6.1 to 8.4, which includes the pH range of sweat. The precision tested at different pH values goes from 2.3 to 3.6 %. When compared to a commercial pH-meter with different samples, the error in the determination was around 2% in almost all the cases. The analytical characterization of the wristband as a whole showed a good fitting (R^2=0.997 in the Boltzmann equation) with a range of use from 6 to 8 and a precision at different pH values from 3.6 to 6.0 %. With an estimated battery life up to 2.63 days in non-continuous sensing mode, the developed system has potential applications in the field of personal health assessment.

Declaration of interests

The authors declare that they have no known competing financial interests or personal relationships that could have appeared to influence the work reported in this paper.

Acknowledgements

This work was founded by Spanish "Ministerio de Economía y Competitividad" (Projects PID2019-103938RB-I00 and CTQ2017-86125-P) and Junta de Andalucía (Projects B-FQM-243-UGR18 and P18-RT-2961). The projects were partially supported by European Regional Development Funds (ERDF).

References

[1] B.W. An, J.H. Shin, S.-Y. Kim, J. Kim, S. Ji, J. Park, Y. Lee, J. Jang, Y.-G. Park, E. Cho, S. Jo, J.-U. Park, Smart Sensor Systems for Wearable Electronic Devices, Polymers (Basel). 9 (2017) 303. doi:10.3390/polym9080303.

[2] I.C. Jeong, D. Bychkov, P.C. Searson, Wearable devices for precision medicine and health state monitoring, IEEE Trans. Biomed. Eng. 66 (2019) 1242–1258. doi:10.1109/TBME.2018.2871638.

[3] MarketsandMarkets, Wearable Fitness Technology Market, (2016). https://www.marketsandmarkets.com/Market-Reports/wearable-fitness-technology-market-139869705.html.

[4] P.J. Chacon, L. Pu, T.H. da Costa, Y.H. Shin, T. Ghomian, H. Shamkhalichenar, H.C. Wu, B.A. Irving, J.W. Choi, A Wearable Pulse Oximeter with Wireless Communication and Motion Artifact Tailoring for Continuous Use, IEEE Trans. Biomed. Eng. 66 (2018) 1505–1513. doi:10.1109/TBME.2018.2874885.

[5] C.M. Boutry, L. Beker, Y. Kaizawa, C. Vassos, H. Tran, A.C. Hinckley, R. Pfattner, S. Niu, J. Li, J. Claverie, Z. Wang, J. Chang, P.M. Fox, Z. Bao, Biodegradable and flexible arterial-pulse sensor for the wireless monitoring of blood flow, Nat. Biomed. Eng. 3 (2019) 47–57. doi:10.1038/s41551-018-0336-5.

[6] F. Riaz, M.A. Azad, J. Arshad, M. Imran, A. Hassan, S. Rehman, Pervasive blood pressure monitoring using Photoplethysmogram (PPG) sensor, Futur. Gener. Comput. Syst. 98 (2019) 120–130. doi:10.1016/j.future.2019.02.032.
[7] F. Güder, A. Ainla, J. Redston, B. Mosadegh, A. Glavan, T.J. Martin, G.M. Whitesides, Paper-Based Electrical Respiration Sensor, Angew. Chemie Int. Ed. 55 (2016) 5727–5732. doi:10.1002/anie.201511805.
[8] M. Manas, A. Sinha, S. Sharma, M.R. Mahboob, A novel approach for IoT based wearable health monitoring and messaging system, J. Ambient Intell. Humaniz. Comput. 10 (2018) 2817–2828. doi:10.1007/s12652-018-1101-z.
[9] G. Liu, C. Ho, N. Slappey, Z. Zhou, S.E. Snelgrove, M. Brown, A. Grabinski, X. Guo, Y. Chen, K. Miller, J. Edwards, T. Kaya, A wearable conductivity sensor for wireless real-time sweat monitoring, Sensors Actuators B Chem. 227 (2016) 35–42. doi:10.1016/j.snb.2015.12.034.
[10] H.Y.Y. Nyein, L. Tai, Q.P. Ngo, M. Chao, G.B. Zhang, W. Gao, M. Bariya, J. Bullock, H. Kim, H.M. Fahad, A. Javey, A Wearable Microfluidic Sensing Patch for Dynamic Sweat Secretion Analysis, ACS Sensors. 3 (2018) 944–952. doi:10.1021/acssensors.7b00961.
[11] W. Gao, S. Emaminejad, H.Y.Y. Nyein, S. Challa, K. Chen, A. Peck, H.M. Fahad, H. Ota, H. Shiraki, D. Kiriya, D.-H. Lien, G.A. Brooks, R.W. Davis, A. Javey, Fully integrated wearable sensor arrays for multiplexed in situ perspiration analysis, Nature. 529 (2016) 509–514. doi:10.1038/nature16521.
[12] A. Martín, J. Kim, J.F. Kurniawan, J.R. Sempionatto, J.R. Moreto, G. Tang, A.S. Campbell, A. Shin, M.Y. Lee, X. Liu, J. Wang, Epidermal Microfluidic Electrochemical Detection System: Enhanced Sweat Sampling and Metabolite Detection, ACS Sensors. 2 (2017) 1860–1868. doi:10.1021/acssensors.7b00729.
[13] M. Parrilla, T. Guinovart, J. Ferré, P. Blondeau, F.J. Andrade, A Wearable Paper- Based Sweat Sensor for Human Perspiration Monitoring, Adv. Healthc. Mater. 8 (2019) 1900342. doi:10.1002/adhm.201900342.
[14] W. Gao, H. Ota, D. Kiriya, K. Takei, A. Javey, Flexible Electronics toward Wearable Sensing, Acc. Chem. Res. 52 (2019) 523–533. doi:10.1021/acs.accounts.8b00500.
[15] G. Xu, C. Cheng, Z. Liu, W. Yuan, X. Wu, Y. Lu, S.S. Low, J. Liu, L. Zhu, D. Ji, S. Li, Z. Chen, L. Wang, Q. Yang, Z. Cui, Q. Liu, Battery- Free and Wireless Epidermal Electrochemical System with All- Printed Stretchable Electrode Array for Multiplexed In Situ Sweat Analysis, Adv. Mater. Technol. 4 (2019) 1800658. doi:10.1002/admt.201800658.
[16] L. Ortega, A. Llorella, J.P. Esquivel, N. Sabaté, Self-powered smart patch for sweat conductivity monitoring, Microsystems Nanoeng. 5 (2019) 3. doi:10.1038/s41378-018-0043-0.
[17] J. Heikenfeld, A. Jajack, B. Feldman, S.W. Granger, S. Gaitonde, G. Begtrup, B.A. Katchman, Accessing analytes in biofluids for peripheral biochemical monitoring, Nat. Biotechnol. 37 (2019) 407–419. doi:10.1038/s41587-019-0040-3.
[18] F.J. Zhao, M. Bonmarin, Z.C. Chen, M. Larson, D. Fay, D. Runnoe, J. Heikenfeld, Ultra-simple wearable local sweat volume monitoring patch based on swellable hydrogels, Lab Chip. 20 (2020) 168–174. doi:10.1039/C9LC00911F.
[19] M. Chung, G. Fortunato, N. Radacsi, Wearable flexible sweat sensors for healthcare monitoring: A review, J. R. Soc. Interface. 16 (2019). doi:10.1098/rsif.2019.0217.
[20] J. Kim, J.R. Sempionatto, S. Imani, M.C. Hartel, A. Barfidokht, G. Tang, A.S. Campbell, P.P. Mercier, J. Wang, Simultaneous Monitoring of Sweat and Interstitial Fluid Using a Single Wearable Biosensor Platform, Adv. Sci. 5 (2018). doi:10.1002/advs.201800880.
[21] T.S. Perry, Wearable sensor detects stress in sweat, IEEE Spectr. 55 (2018) 14–15. doi:10.1109/MSPEC.2018.8449037.
[22] W.P. Nikolajek, H.M. Emrich, pH of sweat of patients with cystic fibrosis, Klin. Wochenschr. 54 (1976) 287–288. doi:10.1007/BF01468925.
[23] M.J. Patterson, S.D.R. Galloway, M.A. Nimmo, Effect of induced metabolic alkalosis on sweat composition in men, Acta Physiol. Scand. 174 (2002) 41–46. doi:10.1046/j.1365-

201x.2002.00927.x.
[24] M.N. Sawka, E.F. Coyle, Influence of Body Water and Blood Volume on Thermoregulation and Exercise Performance in the Heat, Exerc. Sport Sci. Rev. 27 (1999) 167–218. doi:10.1249/00003677-199900270-00008.
[25] V.F. Curto, C. Fay, S. Coyle, R. Byrne, C. O'Toole, C. Barry, S. Hughes, N. Moyna, D. Diamond, F. Benito-Lopez, Real-time sweat pH monitoring based on a wearable chemical barcode micro-fluidic platform incorporating ionic liquids, Sensors Actuators B Chem. 171–172 (2012) 1327–1334. doi:10.1016/j.snb.2012.06.048.
[26] T.D. Noakes, The hyponatremia of exercise., Int. J. Sport Nutr. 2 (1992) 205–228.
[27] T. Kaya, G. Liu, J. Ho, K. Yelamarthi, K. Miller, J. Edwards, A. Stannard, Wearable Sweat Sensors: Background and Current Trends, Electroanalysis. 31 (2019) 411–421. doi:10.1002/elan.201800677.
[28] D. Morris, S. Coyle, Y. Wu, K.T. Lau, G. Wallace, D. Diamond, Bio-sensing textile based patch with integrated optical detection system for sweat monitoring, Sensors Actuators B Chem. 139 (2009) 231–236. doi:10.1016/j.snb.2009.02.032.
[29] N. Lopez-Ruiz, V.F. Curto, M.M.M. Erenas, F. Benito-Lopez, D. Diamond, A.J. Palma, L.F. Capitan-Vallvey, Smartphone-Based Simultaneous pH and Nitrite Colorimetric Determination for Paper Microfluidic Devices, Anal. Chem. 86 (2014) 9554–9562. doi:10.1021/ac5019205.
[30] X. He, T. Xu, Z. Gu, W. Gao, L.-P. Xu, T. Pan, X. Zhang, Flexible and Superwettable Bands as a Platform toward Sweat Sampling and Sensing, Anal. Chem. 91 (2019) 4296–4300. doi:10.1021/acs.analchem.8b05875.
[31] A.J. Bandodkar, P. Gutruf, J. Choi, K. Lee, Y. Sekine, J.T. Reeder, W.J. Jeang, A.J. Aranyosi, S.P. Lee, J.B. Model, R. Ghaffari, C.-J. Su, J.P. Leshock, T. Ray, A. Verrillo, K. Thomas, V. Krishnamurthi, S. Han, J. Kim, S. Krishnan, T. Hang, J.A. Rogers, Battery-free, skin-interfaced microfluidic/electronic systems for simultaneous electrochemical, colorimetric, and volumetric analysis of sweat, Sci. Adv. 5 (2019) eaav3294. doi:10.1126/sciadv.aav3294.
[32] A. Koh, D. Kang, Y. Xue, S. Lee, R.M. Pielak, J. Kim, T. Hwang, S. Min, A. Banks, P. Bastien, M.C. Manco, L. Wang, K.R. Ammann, K.-I. Jang, P. Won, S. Han, R. Ghaffari, U. Paik, M.J. Slepian, G. Balooch, Y. Huang, J.A. Rogers, A soft, wearable microfluidic device for the capture, storage, and colorimetric sensing of sweat, Sci. Transl. Med. 8 (2016) 366ra165-366ra165. doi:10.1126/scitranslmed.aaf2593.
[33] W. Dang, L. Manjakkal, W.T. Navaraj, L. Lorenzelli, V. Vinciguerra, R. Dahiya, Stretchable wireless system for sweat pH monitoring, Biosens. Bioelectron. 107 (2018) 192–202. doi:10.1016/j.bios.2018.02.025.
[34] S. Anastasova, B. Crewther, P. Bembnowicz, V. Curto, H.M. Ip, B. Rosa, G.-Z. Yang, A wearable multisensing patch for continuous sweat monitoring, Biosens. Bioelectron. 93 (2017) 139–145. doi:10.1016/j.bios.2016.09.038.
[35] J. Choi, R. Ghaffari, L.B. Baker, J.A. Rogers, Skin-interfaced systems for sweat collection and analytics, Sci. Adv. 4 (2018) 1–10. doi:10.1126/sciadv.aar3921.
[36] A. Olanrewaju, M. Beaugrand, M. Yafia, D. Juncker, Capillary microfluidics in microchannels: from microfluidic networks to capillaric circuits, Lab Chip. 18 (2018) 2323–2347. doi:10.1039/C8LC00458G.
[37] M. Boada, A. Lazaro, R. Villarino, D. Girbau, Battery-Less NFC Sensor for pH Monitoring, IEEE Access. 7 (2019) 33226–33239. doi:10.1109/ACCESS.2019.2904109.
[38] Y. Lu, K. Jiang, D. Chen, G. Shen, Wearable sweat monitoring system with integrated micro-supercapacitors, Nano Energy. 58 (2019) 624–632. doi:10.1016/j.nanoen.2019.01.084.
[39] R. Kansara, P. Bhojani, J. Chauhan, Designing Smart Wearable to measure Health Parameters, in: 2018 Int. Conf. Smart City Emerg. Technol., IEEE, 2018: pp. 1–5. doi:10.1109/ICSCET.2018.8537314.
[40] A. Alizadeh, A. Burns, R. Lenigk, R. Gettings, J. Ashe, A. Porter, M. McCaul, R. Barrett, D. Diamond, P. White, P. Skeath, M. Tomczak, A wearable patch for continuous monitoring of sweat electrolytes during exertion, Lab Chip. 18 (2018) 2632–2641.

doi:10.1039/c8lc00510a.
[41] S.F. Godek, A.R. Bartolozzi, R. Burkholder, E. Sugarman, C. Peduzzi, Sweat Rates and Fluid Turnover in Professional Football Players: A Comparison of National Football League Linemen and Backs, J. Athl. Train. 43 (2008) 184–189. doi:10.4085/1062-6050-43.2.184.
[42] G.J. Mohr, H. Müller, B. Bussemer, A. Stark, T. Carofiglio, S. Trupp, R. Heuermann, T. Henkel, D. Escudero, L. González, Design of acidochromic dyes for facile preparation of pH sensor layers, Anal. Bioanal. Chem. 392 (2008) 1411–1418. doi:10.1007/s00216-008-2428-7.
[43] J. Morales-Sanfrutos, J. Lopez-Jaramillo, M. Ortega-Muñoz, A. Megia-Fernandez, F. Perez-Balderas, F. Hernandez-Mateo, F. Santoyo-Gonzalez, Vinyl sulfone: a versatile function for simple bioconjugation and immobilization, Org. Biomol. Chem. 8 (2010) 667–675. doi:10.1039/B920576D.
[44] F.J. López-Jaramillo, F. Hernández-Mateo, F. Santoyo-González, Vinyl Sulfone: A Multi-Purpose Function in Proteomics, in: Integr. Proteomics, InTech, 2012. doi:10.5772/29682.
[45] G.J. Mohr, Synthesis of naphthalimide-based indicator dyes with a 2-hydroxyethylsulfonyl function for covalent immobilisation to cellulose, Sensors Actuators B Chem. 275 (2018) 439–445. doi:10.1016/j.snb.2018.07.095.
[46] T. Werner, O.S. Wolfbeis, Optical sensor for the pH 10-13 range using a new support material, Fresenius. J. Anal. Chem. 346 (1993) 564–568. doi:10.1007/BF00321245.
[47] P. Kassal, M. Zubak, G. Scheipl, G.J. Mohr, M.D. Steinberg, I. Murković Steinberg, Smart bandage with wireless connectivity for optical monitoring of pH, Sensors Actuators B Chem. 246 (2017) 455–460. doi:10.1016/j.snb.2017.02.095.
[48] P. Chauhan, C. Hadad, A.H. López, S. Silvestrini, V. La Parola, E. Frison, M. Maggini, M. Prato, T. Carofiglio, A nanocellulose–dye conjugate for multi-format optical pH-sensing, Chem. Commun. 50 (2014) 9493–9496. doi:10.1039/C4CC02983F.
[49] W.T. Suarez, M.O.K. Franco, L.F. Capitán-Vallvey, M.M. Erenas, Chitosan-modified cotton thread for the preconcentration and colorimetric trace determination of Co(II), Microchem. J. 158 (2020) 105137. doi:10.1016/j.microc.2020.105137.
[50] S. Coyle, D. Morris, K.-T. Lau, D. Diamond, F. Di Francesco, N. Taccini, M.G. Trivella, D. Costanzo, P. Salvo, J.-A. Porchet, J. Luprano, Textile sensors to measure sweat pH and sweat-rate during exercise, in: Proc. 3d Int. ICST Conf. Pervasive Comput. Technol. Healthc., ICST, 2009. doi:10.4108/ICST.PERVASIVEHEALTH2009.5957.
[51] M. Caldara, C. Colleoni, E. Guido, V. Re, G. Rosace, Optical monitoring of sweat pH by a textile fabric wearable sensor based on covalently bonded litmus-3-glycidoxypropyltrimethoxysilane coating, Sensors Actuators B Chem. 222 (2016) 213–220. doi:10.1016/j.snb.2015.08.073.
[52] A. Koh, D. Kang, Y. Xue, S. Lee, R.M. Pielak, J. Kim, T. Hwang, S. Min, A. Banks, P. Bastien, M.C. Manco, L. Wang, K.R. Ammann, K.-I. Jang, P. Won, S. Han, R. Ghaffari, U. Paik, M.J. Slepian, G. Balooch, Y. Huang, J.A. Rogers, A soft, wearable microfluidic device for the capture, storage, and colorimetric sensing of sweat, Sci. Transl. Med. 8 (2016) 366ra165-366ra165. doi:10.1126/scitranslmed.aaf2593.